Supplementary Information for:

Polymers in Ionic Liquids and Ionic Liquids in Polymers: Critical Factors for Compatibility and Materialization

Masayoshi Watanabe*

Advanced Chemical Energy Research Center

Institute of Advanced Sciences, Yokohama National University

75-5 Tokiwadai, Hodogaya-ku, Yokohama, Kanagawa 240-8501, Japan

*e-mail: mwatanab@ynu.ac.jp

References in the supporting information are cited in the main text.

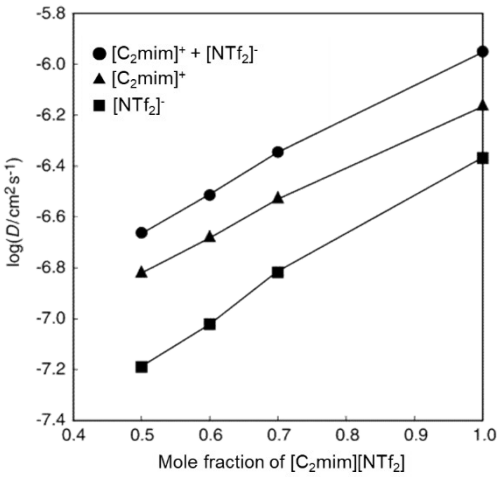

Fig. S1 Diffusivities of $[C_2mim]^+$ cation, $[NTf_2]^-$ anion, and their summation in an ion gel consisting of PMMA network and $[C_2mim][NTf_2]$ as a function of mole fraction of $[C_2mim][NTf_2]$. Reproduced from ref. 6 with permission from Copyright © 2005, American Chemical Society.

Table S1 Compatibility of polyethers in ILs. The indicated temperatures are LCST-type phase separation temperatures (T_c).

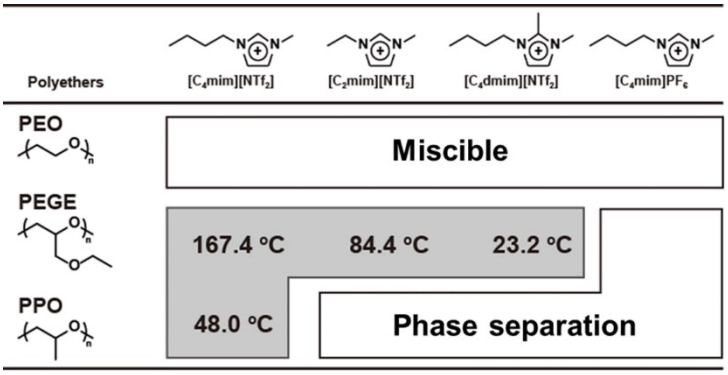

Table S2 Commercially used electrolytes in EDLCs.

	Aqueous electrolyte	Organic electrolyte
Typical example	Dilute sulfuric acid	Et_4NBF_4/PC
Decomposition voltage (per single cell)	1.23 V	~4.0 V
Practical operating voltage	0.6 ~ 0.8 V	2.0 ~ 2.5 V
Features	• Low internal resistance (advantage in power density) • Low cost	• High decomposition voltage (advantage in energy density) • Use of inexpensive metals such as Al as current collector is possible.

Table S3 General comparison of batteries, EDLCs, and electrolytic capacitors.

	Lead-acid battery	EDLC	Eletrolytic capacior
Capacitance (F)	> 10	0.01~10000	< 0.1
Charge time	1~10 h	0.1~20 min	< 1 ms
Discharge time	0.3~3 h	0.1~20 min	< 1 ms
Energy density (Wh kg^{-1})	10~40	0.2~10	<0.1
Power density (W kg^{-1})	50~130	100~2000	<100000
Charge/discharge efficiency (%)	85~90	97~99	>99
Cycle life	200~1000	>100000	>100000

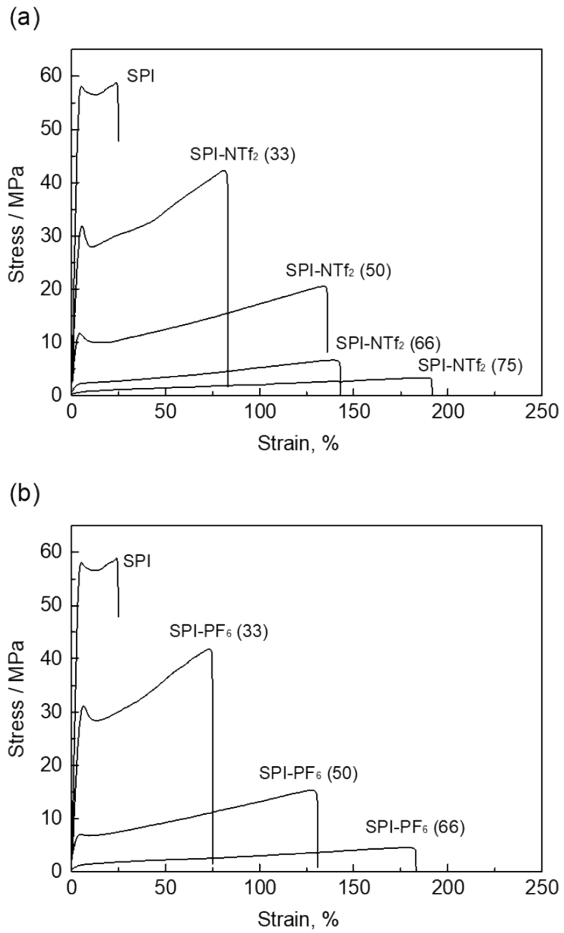

Fig. S2 Stress-strain curves for SPI/$[C_4mim][NTf_2]$ (a) and SPI/$[C_4mim][PF_6]$ composite membranes. Samples were cut into dumbbell shapes (JIS K6251) and measured at a stretching head speed of 1 mm s^{-1}. Reproduced from ref. 83 with permission from Copyright © 2017, Springer Nature.

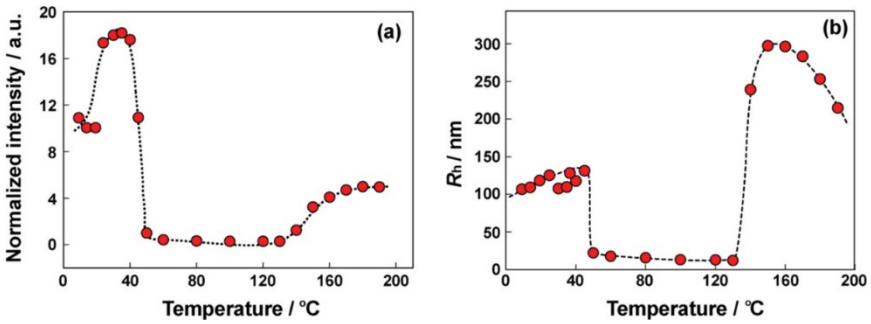

Fig. S3 Temperature dependence for 1 wt % PBnMA-*block*-P(NIPAm-*r*-AAm) solution in $[C_2mim][NTf_2]$: (a) normalized scattering intensity and (b) hydrodynamic radius (R_h) of the solute. Reproduced from ref. 93 with permission from Copyright © 2009, American Chemical Society.

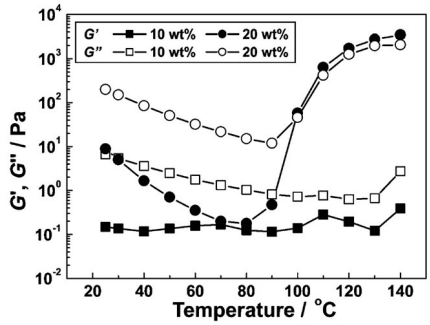

Fig. S4 Variation of dynamic storage (*G*', solid symbol) and loss (*G*", open symbols) moduli of 10 wt% and 20 wt% PBnMA-*block*-PMMA-*block*-PBnMA solutions in $[C_2mim][NTf_2]$ as a function of temperature at a frequency of $\omega = 6.28$ rad s^{-1} and a strain amplitude of $\gamma = 1\%$. Reproduced from ref. 95 with permission from Copyright © 2012, Royal Society of Chemistry.

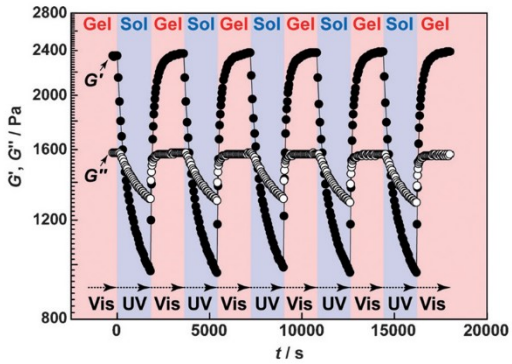

Fig. S5 Reversible sol–gel transition cycle of a 20 wt% P(AzoMA-*r*-NIPAm)-*block*-PEO-*block*-P(AzoMA-*r*-NIPAm) solution in $[C_4mim][PF_6]$ by alternately switching between UV and visible-light irradiation at 53.8 °C. Period of UV and visible-light irradiation indicated by arrows. Reproduced from ref. 100 with permission from Copyright © 2015, Wiley.